A snapback suppressed reverse-conducting IGBT with uniform temperature distribution*

Chen Wei-Zhong(陈伟中)†, Li Ze-Hong(李泽宏), Zhang Bo(张 波), Ren Min(任 敏), Zhang Jin-Ping(张金平), Liu Yong(刘 永), and Li Zhao-Ji(李肇基)

State Key Laboratory of Electronic Thin Films and Integrated Devices, University of Electronics Science and Technology of China, Chengdu 610054, *China*

(Received 7 April 2013; revised manuscript received 8 June 2013; published 3 December 2013)

A novel reverse-conducting insulated-gate bipolar transistor (RC-IGBT) featuring a floating P-plug is proposed. The P-plug is embedded in the n-buffer layer to obstruct the electron current from flowing directly to the n-collector, which achieves the hole emission from the p-collector at a small collector size and suppresses the snapback effectively. Moreover, the current is uniformly distributed in the whole wafer at both IGBT mode and diode mode, which ensures the high temperature reliability of the RC-IGBT. Additionally, the P-plug acts as the base of the N-buffer/P-float/N-buffer transistor, which can be activated to extract the excessive carriers at the turn-off process. As the the simulation results show, for the proposed RC-IGBT, it achieves almost snapback-free output characteristics with a uniform current density and a uniform temperature distribution, which can greatly increase the reliability of the device.

Keywords: reverse-conducting insulated-gate bipolar transistor, snapback, temperature reliability

PACS: 85.30.De, 85.30.Pq, 85.30.Tv **DOI:** 10.1088/1674-1056/23/1/018505

1. Introduction

Insulated-gate bipolar transistors (IGBTs) have already become one of the mainstream power devices in medium–high voltage applications and their use is continuously expanding due to the improvements in the device structure.[1–3] A reverse conducting insulated-gate bipolar transistor (RC-IGBT) is obtained by incorporating an IGBT and a diode in a monolithic chip and introducing an n-collector in the backside of the IGBT.[4–7] Such a structure could offer a more compact circuit solution. However, several unreliabilities, such as an undesirable snapback, which can prevent the device from fully turning on[8–10], and a non-uniform distributed current, which can cause the device to overheat, are observed. Then many methods have been proposed to suppress the snapback, such as improving the resistance of the n-buffer ($R_{\rm buffer}$),[11,12] diminishing the drift resistance $R_{\rm drift}$ by adopting a super junction (SJ-RC-IGBT)[13–16] and diminishing the junction field-effect transistor (JFET) resistance $R_{\rm JFET}$ by adopting a trench metal-oxide-semiconductor (MOS) structure (TFS-RC-IGBT). The cause of the non-uniform distributed current for the conventional RC-IGBT is that a large collector size is needed to ensure the hole emission and the conductivity modulation usually only occurs at the p-collector part. In recent years, most research has mainly focused on the snapback. The bi-mode insulating gate transistor (BIGT) is a simple way to suppress the drawback without extra masks.[17–19] However, due to the difference of the hole emission efficiency between the IGBT and RC-IGBT parts, the current is non-uniform, which may cause the device to overheat at some local areas, resulting in a destructive failure for the power device.

In this paper, a novel RC-IGBT with a floating P-plug is proposed to suppress the snapback and to realize the current uniformity and enhance the temperature reliability of the RC-IGBT.

2. Device structures and theoretical analysis

2.1. Device structures

Figure 1 shows the BIGT structure and the proposed RC-IGBT with a floating P-plug. The n-collector regions on the backside enable the IGBT to conduct a current when the collector–emitter is reversely biased. The n-collector regions act as a cathode emitter, while the p-body of the IGBT near the front side acts as an anode emitter of a diode integrated into the chip in this way. In Figs. 1(a) and 1(b), they have the same structure parameters except for the collector region. The main parameters of the IGBTs are listed in Table 1. The thickness and the doping concentration of the N-drift region are 120 μm and 7×10^{13} cm^{-3}, respectively, for a blocking capability of 1200 V. The carrier lifetime and the ambient temperature are 10 μs and 300 K, respectively. The ratio for n-collector length $L_{\rm n}$ and p-collector length $L_{\rm p}$ is set at 1:4 for all the RC-IGBTs. The $L_{\rm size}$ of the BIGT is 600 μm; the device is formed by an RC-IGBT part and a conventional IGBT part. For the proposed structure, due to the introduction of the

*Project supported by the National Science and Technology Major Project, China (Grant No. 2011ZX02504-003), the National Natural Science Foundation of China (Grant No. 61076082), and the Fundamental Research Funds for the Central Universities, China (Grant No. ZYGX2011J024).

†Corresponding author. E-mail: cwz@cqu.edu.cn

© 2014 Chinese Physical Society and IOP Publishing Ltd

p-plug in the n-buffer layer, the electron path in the n-buffer is blocked and the electrons will store at the n-buffer layer upon the p-collector. Thus the device can be seen as a combination of a diode part and a conventional IGBT part. Different from the conventional RC-IGBT, the two parts can work independently.

Table 1. Device specifications.

Parameter	Proposed	Conventional RC-IGBT	BIGT
Single MOS cell size, $L_M/\mu m$	15	15	15
Wafer thickness, $W/\mu m$	120	120	120
N-drift doping, $N_B/10^{13}$ cm^{-3}	7	7	7
N-buffer thickness, $d_{n-buffer}/\mu m$	4	4	4
N-buffer doping, $N/10^{16}$ cm^{-3}	2	2	2
Collector cell length, $L_{size}/\mu m$	75	300	600
p-collector thickness/μm	1	1	1
p-collector doping/10^{18} cm^{-3}	5	5	5
p-collector length, $L_p/\mu m$	58	240	480
n-collector length, $L_n/\mu m$	15	60	120
n-collector thickness/μm	1	1	1
n-collector doping/10^{18} cm^{-3}	5	5	5
Oxide trench depth/μm	2	–	–
Oxide trench width/μm	2	–	–
Floating P-plug depth, $d/\mu m$	3	–	–
Floating P-plug width, $w/\mu m$	2	–	–
Floating P-plug doping, $N_p/10^{16}$ cm^{-3}	2	–	–

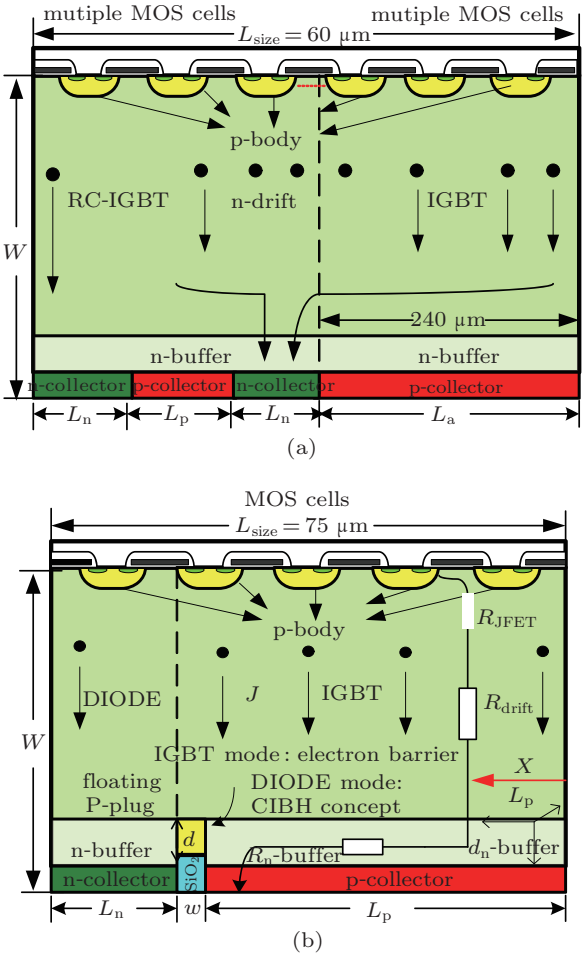


Fig. 1. (color online) Device structures of (a) the BIGT and (b) the proposed RC-IGBT with floating P-plug .

2.2. Theoretical analysis

Figure 2 shows the schematic diagram of the snapback point and the holding point. Equations (1)–(6) show the relationship of the key parameters of the RC-IGBTs for initiating the hole injection

$$V_{supply} = V_{n-buffer} + V_{drift} + V_{JFET}, \tag{1}$$

$$V_{n-buffer} = R\int_0^{L_p} J\,dx + I\int_0^{L_p} R\,dx = 2JL_P^2R = 2JL_P^2/Nq\mu d_{n-buffer}. \tag{2}$$

At this point, the device conduction changes from unipolar mode to bipolar mode. On the other hand, the extent of the snapback, as illustrated in Fig. 2, is determined by the ratio of the drift resistance to the anode resistance, snapback point

$$V_{SB} = I(R_{n-buffer} + R_{drift} + R_{JFET}), \tag{3}$$

$$V_{SB} = 0.7\left(1 + \frac{R_{drift} + R_{JFET}}{R_{n-buffer}}\right); \tag{4}$$

holding point

$$V_H \approx V_{SB} - IR_{drift}, \tag{5}$$

$$\Delta V_{SB} = V_{SB} - V_H = \frac{0.7R_{drift}Nq\mu_n d_{n-buffer}}{L_p}; \tag{6}$$

where V_{supply} is the total voltage, $V_{n-buffer}$ is the anode voltage across the n-buffer resistance $R_{n-buffer}$, V_{drift} is the voltage across the drift resistance R_{drift}, V_{JFET} is the voltage across the JFET resistance R_{JFET}, J is the current density, R is the sheet resistance along the X axis, L_p is the length of the p-collector, N and $d_{n-buffer}$ are the doping density and width of the electron channel of the n-buffer, respectively, q is the basic charge, V_{SB} and V_H are the snapback point and the holding point, respectively, as illustrated in Fig. 3. From Eqs. (2) and (6), it can be seen that the n-buffer voltage drop $V_{n-buffer}$ is directly proportional to length L_p and inversely proportional to $d_{n-buffer}$. For ΔV_{SB}, the situation is just contrary to $V_{n-buffer}$.

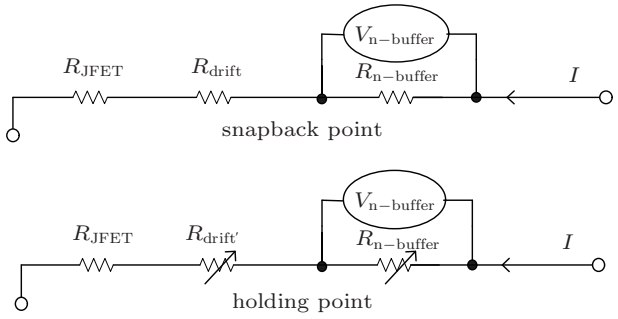


Fig. 2. Schematic diagram of the snapback point and the holding point.

In the following section, we will firstly study the forward conduction property and the turn-off property at IGBT mode; then we will discuss the reverse conduction properties and the reverse recovery property at diode mode; finally, we will show the trade-off property for all the RC-IGBTs.

3. Simulation results and discussion

3.1. Forward conduction property at IGBT mode

Figure 3(a) shows the forward conduction characteristics of the proposed RC-IGBT, the conventional RC-IGBT and the BIGT with different collector sizes. For the conventional RC-IGBT with collector size $L_{\rm size} = 75$ μm, it works as a VDMOS as the voltage drop $V_{\rm n-buffer}$ cannot reach 0.7 V. From Eq. (2), we can increase $V_{\rm n-buffer}$ by lengthening the p-collector size $L_{\rm p}$. When the total collector size $L_{\rm size}$ reaches 300 μm, it can work at bipolar mode and the snapback is evident, $\Delta V_{\rm SB}$ is 1.5 V. Moreover, from Figs. 4(b-1) and 4(b-2), we find that the current and temperature distributions are non-uniform. For the BIGT, the total collector size $L_{\rm size}$ is set at 600 μm to suppress the snapback, the extent of snapback $\Delta V_{\rm SB}$ is 1.2 V. According to Eq. (6), to eliminate $\Delta V_{\rm SB}$ completely, $L_{\rm p}$ should be set at infinity. For example, in Ref. [18], the total collector size $L_{\rm size}$ is set high, up to 2500 μm. On the other hand, the BIGT is separated by RC-IGBT and conventional IGBT parts, the IGBT part has a much higher hole emission efficiency than the RC-IGBT part, which induces the concentration of the current at the IGBT part and consequently results in the temperature overheating at local areas, as shown in Figs. 4(c-1) and 4(c-2). For the proposed RC-IGBT, the floating P-plug embedded in the n-buffer offers a barrier to the electron current, it can work at bipolar mode despite the collector size $L_{\rm size} = 75$ μm, $\Delta V_{\rm SB}$ is only 0.2 V. When $L_{\rm size} = 300$ μm, $\Delta V_{\rm SB}$ is completely eliminated. Moreover, in Figs. 4(a-1) and 4(a-2), the current and temperature distributions are very uniform.

Figure 3(b) shows the $d_{\rm n-buffer}$ influencing on the snapbacks. It can be seen that $\Delta V_{\rm SB}$ decreases from 3.5 V to 0.2 V when $d_{\rm n-buffer}$ decreases from 3 μm to 0 μm. According to Eq. (6), the snapback can be completely eliminated by decreasing $d_{\rm n-buffer}$ to zero. So the floating P-plug can suppress the snapback effectively. When the height of the p-plug equals the width of the n-buffer, the electron channel is almost completely obstructed.

Figure 3(c) shows the doping of the float P-plug influencing on the snapbacks. It can be seen that $\Delta V_{\rm SB}$ decreases from 0.4 V to 0.18 V when the doping increases from 1×10^{15} cm^{-3} to 4×10^{16} cm^{-3}.

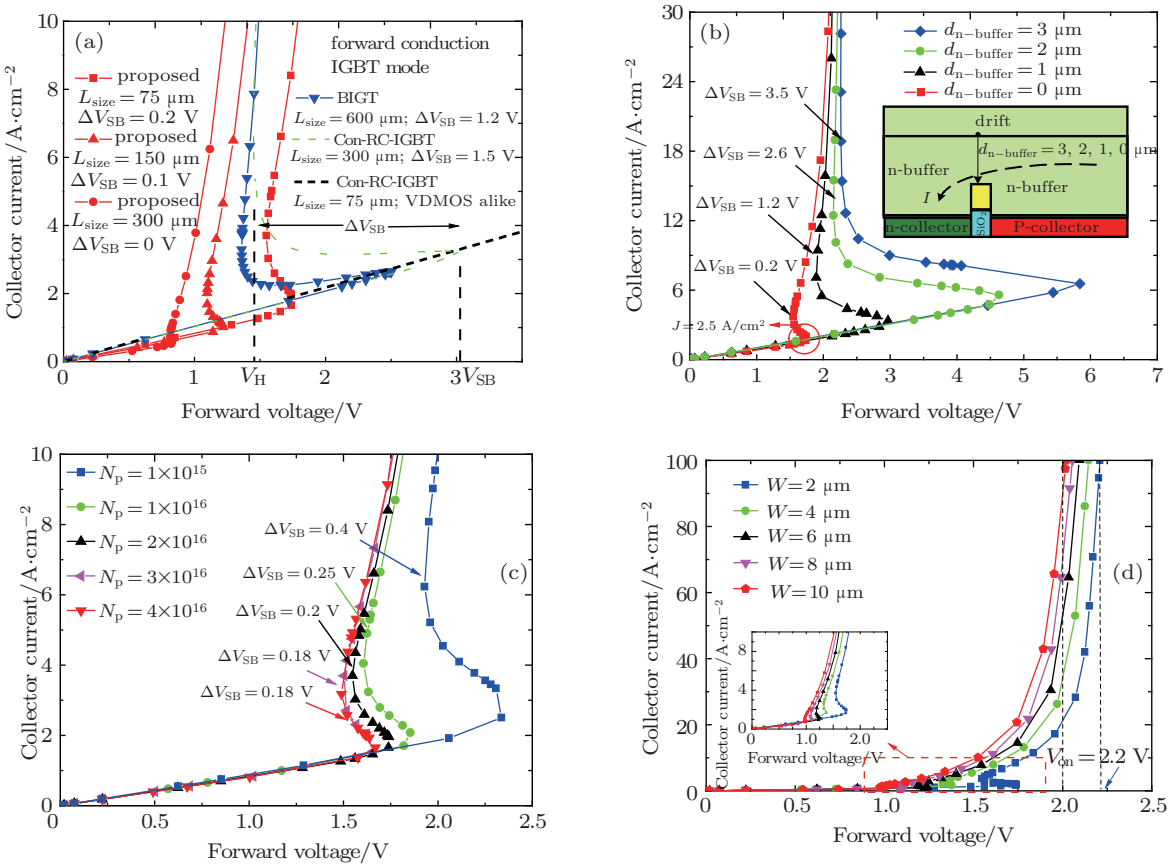


Fig. 3. (color online) (a) Comparison of the forward conduction characteristics for the BIGT, the conventional RC-IGBT and the proposed RC-IGBT with floating P-plug at different collector sizes. (b) Dependencies of forward conduction characteristics and $\Delta V_{\rm SB}$ $(= V_{\rm SB} - V_{\rm H})$ on $d_{\rm n-buffer}$. Here, $V_{\rm SB}$ is the turn-over voltage of the snapback and $V_{\rm H}$ is the minimum collector voltage after snapback. (c) Dependencies of forward conduction characteristics and $\Delta V_{\rm SB}$ on the doping of the floating P-plug. (d) Dependencies of forward conduction characteristics and $\Delta V_{\rm SB}$ on the width of the floating P-plug.

Figure 3(d) shows the width of the float P-plug influencing on the snapbacks. It can be seen that ΔV_{SB} decreases slowly as the width increases from 2 μm to 10 μm. Moreover, the forward voltage drop is 2.2 V for the proposed RC-IGBT at the current density of 100 A/cm^2.

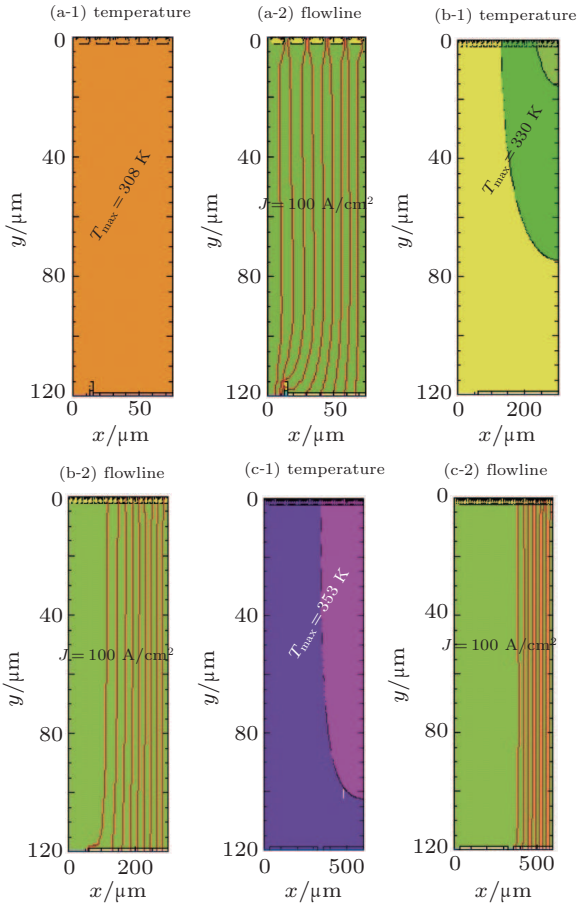


Fig. 4. (color online) The 2D temperature and current distributions for (a) the proposed RC-IGBT, (b) the conventional RC-IGBT and (c) the BIGT at the current density of 100 A/cm^2, the ambient temperature is set at 298 K.

3.2. Turn-off property at IGBT mode

The turn-off current waveforms for the IGBTs under a clamped inductive load are shown in Fig. 5. For the proposed structure, except for the n-collector, the floating P-plug embedded in the n-buffer layer acts as the base of the N-buffer/P-float/N-buffer transistor to extract the excessive carriers. For the conventional RC-IGBT and BIGT, although they have n-collectors for extracting electrons, they need much bigger collector sizes to attain the same forward voltage drop and suppress the NDR regime. Moreover, the majority of the excessive carriers are accumulated upon the p-collector area and it is hard for the p-collector to extract them out, which induces the slowness of the turn-off process. Additionally, the non-uniform current distribution will induce an electric field and depletion layer fluctuation between the diode part and the IGBT part, as shown in Figs. 6(b) and 6(c). For the proposed RC-

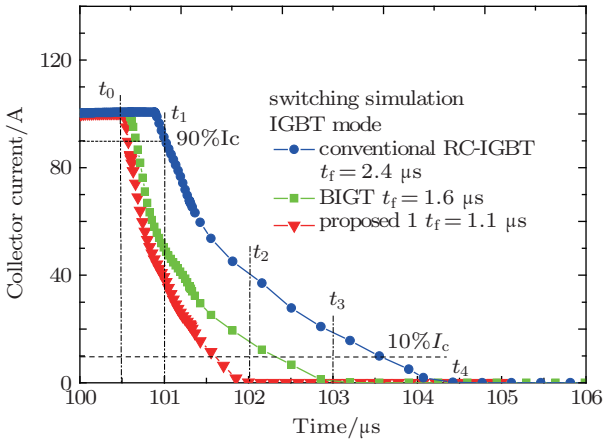


Fig. 5. (color online) Turn-off current waveforms of the conventional RC-IGBT, the BIGT and the proposed RC-IGBT under a clamped inductive load (R_g = 10 Ω, L = 10 μH, line voltage V_c = 600 V, the life time of carriers is t = 10 μs).

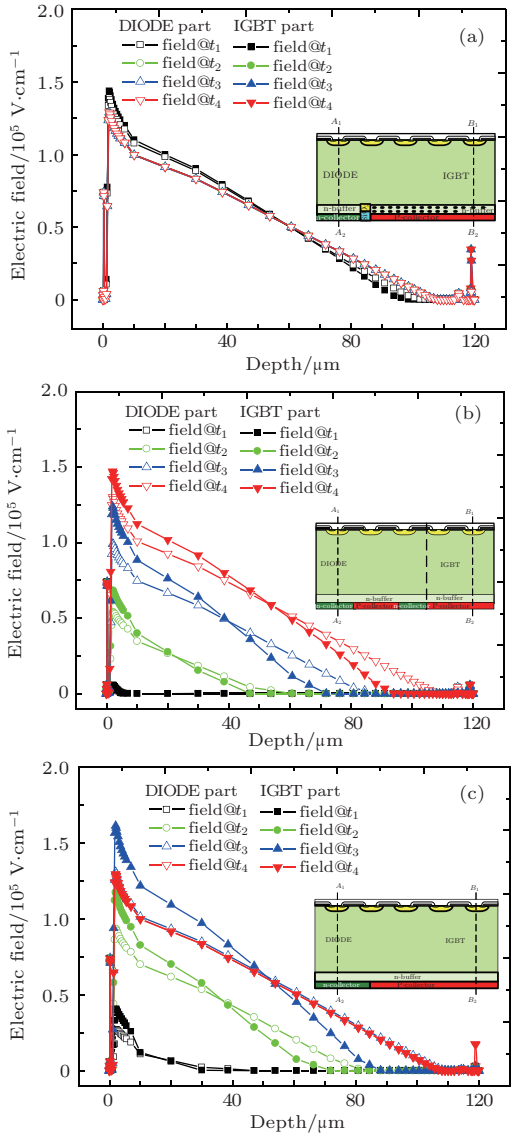


Fig. 6. (color online) Comparison of the evolution of the electric field during turn-off process during the time from t_1 to t_4, as shown in Fig. 5 for (a) the proposed RC-IGBT, (b) the BIGT, (c) the conventional RC-IGBT (the electric field of the diode part is along cut line A_1A_2, the electric field of the IGBT part is along cut line B_1B_2).

IGBT, the current is uniformly distributed during the whole turn-off process; the electric field and depletion layer are almost the same between the diode part and the IGBT part, as shown in Fig. 6(a).

3.3. Reverse conduction property at diode mode

Figure 7 shows the reverse conduction characteristics of the IGBTs at diode mode. The voltage drops are 0.88 V, 1.04 V, 1.08 V and 1.26 V for the conventional PIN, the proposed RC-IGBT, the conventional RC-IGBT and the BIGT, respectively, at 100 A/cm^2. The current and temperature distributions are also investigated at the current density of 300 A/cm^2 because the RC-IGBT may work at momentary high currents during reverse conduction. From Figs. 8(a-1) and 8(a-2), we can see that due to the small collector cell size for the proposed RC-IGBT, the current density and temperature are evenly distributed. In Figs. 8(b-1) and 8(b-2), the non-uniform distribution of the current density induces an extrusive temperature in the conventional RC-IGBT. This phenomenon is more evident in Figs. 8(c-1) and 8(c-2) for the BIGT.

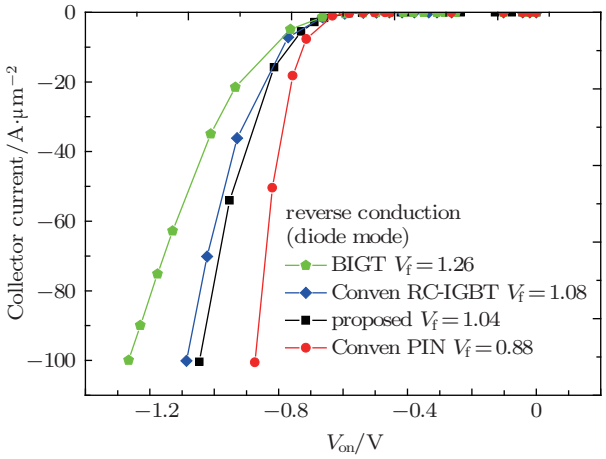


Fig. 7. (color online) Reverse conduction characteristics of the proposed RC-IGBT, the conventional RC-IGBT and the BIGT at diode mode.

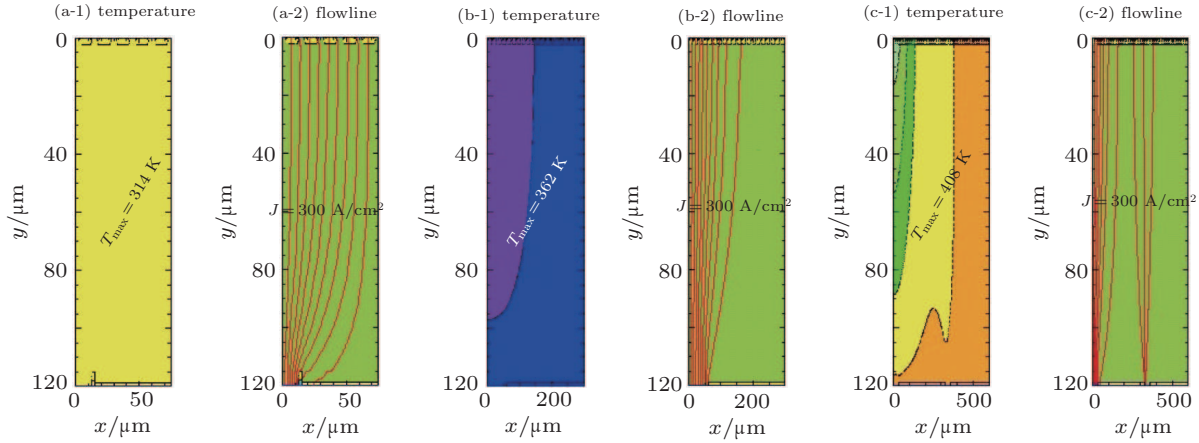


Fig. 8. (color online) The 2D current flow line and temperature distribution for (a) the proposed RC-IGBT, (b) the conventional RC-IGBT and (c) the BIGT at the same current density of 300 A/cm^2, the ambient temperature is set at 298 K.

3.4. Reverse recovery property at diode mode

Figure 9 shows the comparison of the reverse recovery current waveforms of the conventional PIN diode and other RC-IGBTs at diode mode. For all the RC-IGBTs at the reverse recovery state, the passing electrons flowing towards the n-collector regions induce a large potential across the PN junction and force a controlled level of field charge extraction (FCE) (or hole injection) from the p-collector into the base.[20] That is the cause for the soft recovery of the RC-IGBTs at the diode mode. Due to the introduction of the floating P-plug in the n-buffer layer, the proposed RC-IGBT will work as the controlled injection of backside holes (CIBH) concept diode,[21,22] which brings in a soft factor S up to 7. For the conventional PIN diode, due to the lack of the p-collector, the depletion layer increases abruptly in the n-drift. The carriers stored in the base will be extracted at a very short time. That is the cause for the snappy recovery of the PIN diode.[23]

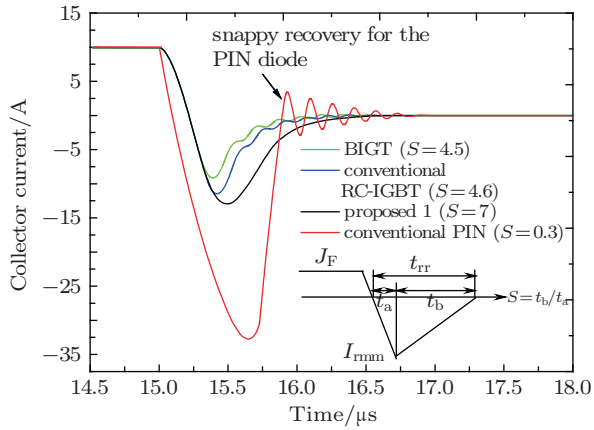


Fig. 9. (color online) Comparison of reverse recovery waveforms of the conventional PIN diode and others RC-IGBTs at diode mode, where $I_F = 10$ A, $V_{cc} = 600$ V, $L = 6$ μH, $\mathrm{d}i/\mathrm{d}t = 200$ A/μs.

3.5. Trade-off property between forward conduction and turn-off loss

The trade-off between the forward voltage drop and turn-off loss $E_{\rm off}$ is comparatively illustrated in Fig. 10. It is obvious that the trade-off curve of the proposed RC-IGBT lies below those of the others. The proposed RC-IGBT has the lowest turn off loss compared with the other RC-IGBTs at the same forward voltage drop, or the proposed RC-IGBT has the lowest forward voltage drop compared with the other RC-IGBTs at the same turn off loss.

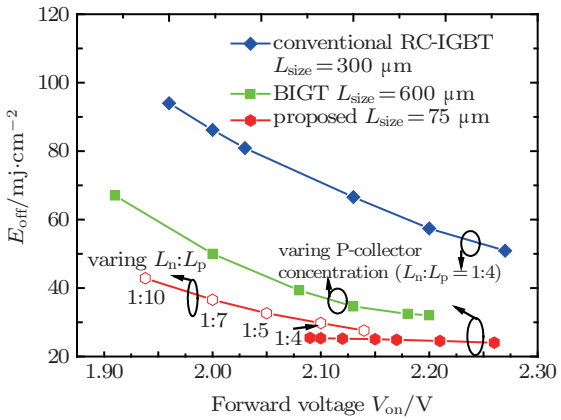


Fig. 10. (color online) Comparison of trade-off between the forward voltage drop and the turn-off loss for the conventional RC-IGBT, the BIGT and the proposed RC-IGBT with float P-plug.

4. Conclusion

An RC-IGBT with a floating P-plug has been presented and investigated in detail. An almost snapback-free RC-IGBT with 75- μm-length collector cell, 2.2-V forward voltage drop, 34.6-mJ/cm^2 turn-off loss and 1.04-V reverse voltage drop of the integrated FWD at 100 A/cm^2 is obtained. As the simulation results show, the new structure not only suppresses the snapback at the IGBT mode but also has superior reverse conduction characteristics at the diode mode; more importantly, due to the uniformity of the current density, the temperature reliability of the RC-IGBT can be greatly improved at large current densities.

References

[1] Luo X R, Yao G L, Chen X, Wang Q, Ge R and Florin U 2011 *Chin. Phys. B* **20** 028501
[2] Hu S D, Wu L J, Zhou J L, Gan P, Zhang B and Li Z J 2012 *Chin. Phys. B* **21** 027101
[3] Zhang J P, Li Z H, Zhang B and Li Z J 2012 *Chin. Phys. B* **21** 068504
[4] Napoli E, Spirito P, Strollo A G M, Frisina F, Fragapane L and Fagone D 2002 *Electron Device Lett.* **23** 532
[5] Takahashi H, Yamamoto A, Aono A and Minato T 2004 *ISPSD* p. 133
[6] Ruthing H, Hille F, Niedernostheide F J, Schulze H J and Brunner B 2007 *ISPSD* p. 89
[7] Rahimo M, Schlapbach U, Kopta A, Vobecky J, Schneider D and Baschnagel A 2008 *ISPSD* p. 68
[8] Chen W, Zhang B and Li Z 2012 *Electron Device Lett.* **31** 467
[9] Jiang, H, Zhang B, Li Z and Dong B 2012 *Electron Device Lett.* **33** 417
[10] Kumar D, Sweet M, Vershinin K, Ngwendson L and Narayanan E M S 2007 *ISPSD* p. 161
[11] Voss S, Niedernostheide F J and Schulze H J 2008 *ISPSD* p. 169
[12] Hsu W C W, Udrea F, Hsu, H Y and Lin W C 2010 *ISPSD* p. 149
[13] Antoniou M, Udrea F and Bauer F 2007 *ISPSD* p. 101
[14] Antoniou M, Udrea F, Bauer F and Nistor I 2010 *ISPSD* p. 153
[15] Antoniou M, Udrea F, Bauer F and Nistor I 2011 *Electron Devicesl.* **58** 769
[16] Minato T, Aono S, Uryu K and Yamaguchi T 2012 *ISPSD* p. 137
[17] Rahimo M, Kopta A, Schlapbach U, Vobecky J, Schnell R and Klaka S 2009 *ISPSD* p. 283
[18] Storasta L, Kopta A and Rahimo M 2012 *ISPSD* p. 391
[19] Storasta L, Rahimo M, Bellini M, Kopta A, Vemulapati U R and Kaminski N 2011 *ISPSD* p. 56
[20] Rahimo M and Kopta A 2005 *ISPSD* p. 1
[21] Chen M, Lutz J, Domeij M, Felsl H P and Schulze H J 2006 *ISPSD* p. 9
[22] Felsl H P, Pfaffenlehner M, Schulze H, Biermann J, Gutt T, Schulze H J, Chen M and Lutz J 2008 *ISPSD* p. 173
[23] Lutz J, Baburske R, Chen M, Heinze B, Domeij M, Felsl H P and Schulze H J 2009 *Electron Devices.* **56** 2825